J Mater Sci (2010) 45:1655–1662
DOI 10.1007/s10853-009-4143-y

Microstructure and mechanical properties of ultrafine grain ZK60 alloy processed by equal channel angular pressing

Yunbin He · Qinglin Pan · Yinjiang Qin · Xiaoyan Liu · Wenbin Li

Received: 22 October 2009 / Accepted: 17 December 2009 / Published online: 30 December 2009

Abstract The microstructure evolution and tensile properties of ZK60 magnesium alloy after equal channel angular pressing (ECAP) have been investigated. The results show that the two-step ECAP process is more effective in grain refinement than the single-step ECAP process due to the lower deformation temperature, a mean grain size of ~0.8 μm was obtained after two-step ECAP process at 513 K for four passes and 453 K for four passes. The EBSD examination reveals that ZK60 alloy after two-step ECAP process exhibits a more homogeneous grain size and misorientation distribution than single-step ECAP process. Both alloys after ECAP process present similar strong {0002} texture. The tensile strength of two-step ECAP alloy has also been improved compared with the single-step ECAP alloy. The strengthening effect was mainly ascribed to grain refinement.

Introduction

Magnesium-based alloys have high potential as structural materials due to their low density. However, the application of these alloys has been limited because of their poor formability and limited ductility at room temperature, which rooted in the intrinsic hexagonal closed-packed (HCP) crystal structure. Grain refinement is an effective procedure for achieving high strength and ductility at room temperature together with possible superplastic forming capabilities at elevated temperatures. It is now well established that remarkable grain refinement can be achieved by introducing equal channel angular pressing (ECAP) to the face-center cubic alloys such as aluminum and copper alloys [1–10]. Those alloys processed by ECAP exhibit enhanced strength and good ductility. Though the same successful results have been obtained on magnesium alloys [11–13], the grain refinement introduced by ECAP processing has been less effective on magnesium alloys compared with aluminum alloys. This is mainly ascribed to the high deformation temperature of the ECAP processing for magnesium alloys, which leads to easy dynamic recovery and rapid grain growth.

In order to lower the deformation temperature, attempts have been carried out in the past few years. Xia et al. [14] have introduced back pressure to ECAP process on AZ31 alloy, which generates a compressive hydrostatic pressure to the sample and reduces the possibility of crack initiation and growth. With back pressure, the ECAP can be successfully performed at as low as 373 K on AZ31 magnesium alloy. The nature of the initial structure of the starting material is also critical to the microstructure evolution during the ECAP processing. As fine grains are more adjustable to the severe plastic deformation, a fine-grained starting material might exhibit high formability. Watanabe et al. [15] have successfully obtained a fine-grained ZK60 alloy by ECAP at 433 K for eight passes using a starting material with 5 μm and the ECAP processed ZK60 alloy exhibited low temperature superplasticity. Matsubara et al. [16] established a method designated as EX-ECAP where the billets were subjected to extrusion before ECAP processing. The extrusion processing refined the grain size of ZK60 alloy to 12 μm which facilitated the subsequent low temperature ECAP deformation at 473 K. Jin et al. [17] also developed a two-step ECAP process on AZ31 alloy where the sample was first processed by ECAP at high temperature and subsequently ECAP at low temperature.

Y. He (✉) · Q. Pan · Y. Qin · X. Liu · W. Li
Department of Materials Science and Engineering, Central South University, Changsha 410083, China
e-mail: mcdonlean@gmail.com

The first step at high temperature can produce a homogenous fine-grained structure, which can facilitate the low temperature ECAP process at the second step.

Figueiredo and Langdon [18] reported a critical grain size of the starting material, which significantly influence the homogeneousness of the ultimate microstructure of the ECAP processed magnesium alloys. When the grain size of the starting material is small than the critical value, it is more easily to attain a homogenous structure, otherwise a bimodal or necklace-like structure is formed. The critical grain is also dependent upon the pressing temperature. When the pressing temperature is increased to activate non-basal slip, the critical grain size becomes larger.

In order to avoid obvious cracking, most of the ECAP process on ZK60 alloy is usually conducted at a temperature not less than 473 K [18–23]. However, there is a potential to produce an ultrafine grain structure for ZK60 alloy by low temperature ECAP processing. In the present investigation, the two-step ECAP processing was applied on a ZK60 magnesium alloy in order to refine the grain size and improve the mechanical properties. The microstructure evolution during the two-step ECAP processing was investigated.

Experimental

The material used in the present study was a commercially available magnesium alloy ZK60 (5.6 wt% Zn, 0.6 wt% Zr). The ZK60 alloy was supplied as-extruded bar. Rods of Φ20 × 100 mm were machined out from the extruded bar and solution treated at 703 K for 10 h. The billets were pressed in an ECAP die with Φ20 mm channel, 90° intersection angle, and a 20° curvature on the outer side of the channel intersection which imposes a strain of ~1 for each pass.

For single-step ECAP process experiments, samples were pressed through the die for four and eight passes at 513 K. For two-step ECAP process experiments, samples were first pressed at 513 K for four passes and then pressed at 453 K for four passes. The pressing speed was controlled at about ~20 mm/min. All the ECAP process experiments were carried out via route B_c, where the sample was rotated 90° in the same sense along the longitudinal axis. A mixture of graphite powder and engine oil was used as the lubricant for the ECAP.

After the ECAP processing, dog-bone shape tensile specimens with gauge dimensions of 2 × 3 × 5 mm were machined from the processed rod samples, with tensile axis lying along the longitudinal axes of the ECAP processed samples. Tensile tests were carried out on an MTS universal testing machine at a nominal strain rate of 1.0×10^{-3} s^{-1} at room temperature.

The microstructure of the ECAP processed alloy was characterized by the optical microscopy, scanning electron microscopy (SEM), and transmission electron microscopy (TEM). The specimens for optical microscopy examination were mechanically polished down to 1 μm and then etched with a solution containing 1 g oxalic acid, 1 mL nitric acid, 1 mL acetic acid, and 100 mL distilled water. The specimens for TEM observation were first mechanically polished and then electro-polishing using a Tenupol 5 jet polishing unit with electrolyte containing 11.4 g magnesium perchloric, 5.8 g lithium chloride, 500 mL methanol, and 100 mL buthyloxy-ethanol at −45 °C, 50 V. The TEM examination was carried out on a Tecnai G^2 20 transmission electron microscope operating at 200 kV. The electron back scatter diffraction (EBSD) was carried out using an EDAX EBSD detector mounted in the SEM. The sample preparation used in EBSD was the same as TEM but without perforation. The EBSD data was analyzed using the OIM software provided by EDAX.

Results

Optical microstructure

Figure 1 shows the optical microstructure of the as-solution ZK60 alloy and samples after ECAP process. It can be seen from Fig. 1a that the as-solution alloy exhibits a bi-modal structure, with coarse elongated grains of ~200 μm and fine recrystallized grains of ~10 μm around the coarse grains, which was described as necklace-like structure in the previous researches. Figure 1b, c shows the grain structure after single-step ECAP at 513 K. It is evident that significant grain refinement was obtained after ECAP processing at 513 K for four passes. The grains are nearly equiaxed with reduced grain size of ~1.8 μm. However, the grain size structure still exhibit a bi-modal structure which consists of few coarse grains of ~10 μm embedded in relatively large amount of fine grains. The bi-model structure might be attributed to the inhomogeneous structure of the starting material. With the increasing pressing pass, the grain structure became more homogenous after eight passes, and the grain size was slightly reduced to ~1.6 μm. After two-step ECAP, the grain size was further reduced. The grain size was too small to be distinguished by optical microscopy. A closer investigation using SEM revealed that the grain size of the two-step ECAP sample was ~0.8 μm.

EBSD examination

Since the two-step ECAP process introduces a remarkable grain refinement to the ZK60 alloy, the grain

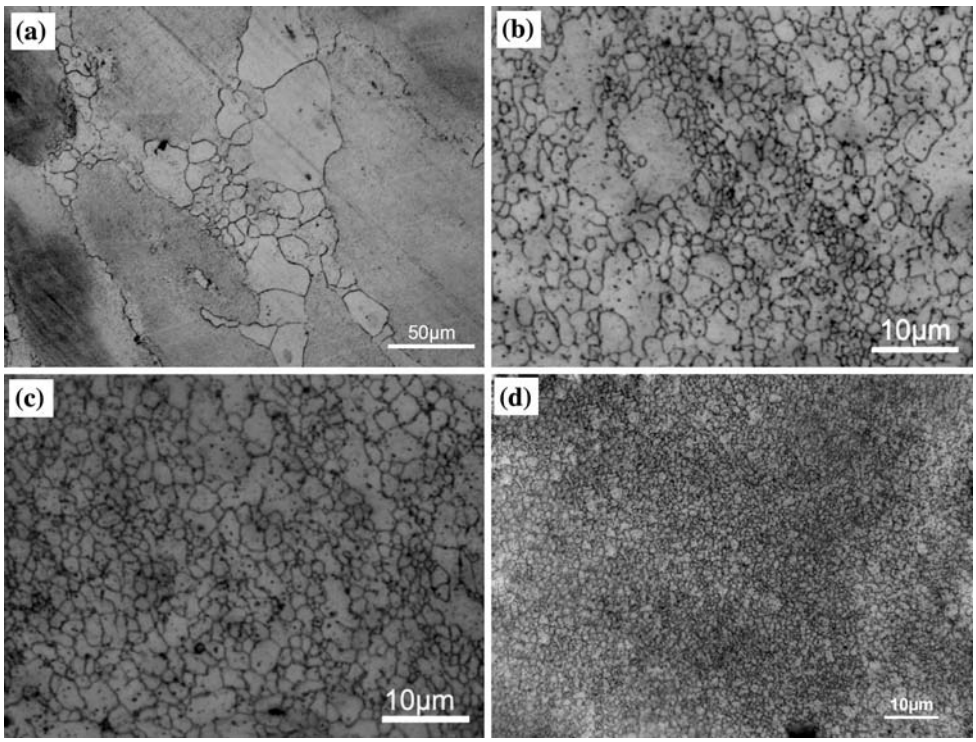

Fig. 1 Optical microstructure of as-solution ZK60 alloy (**a**) and after single-step ECAP at 513 K for four passes (**b**) and eight passes (**c**) and after two-step ECAP at 513 K for four passes and 453 K for four passes (**d**)

structure could not easily be distinguished by optical microscopy. The EBSD method was utilized to characterize the grain structure of the two-step ECAP processed alloy. The results were compared to that of single-step ECAP at 513 K for eight passes. The obtained EBSD orientation maps of the ECAP processed alloys are shown in Fig. 2. The different colors are assigned to different grain orientations. The distinguishing color of two grains means that the orientation between two grains is large. The grain size distribution is charted in Fig. 3. After two-step ECAP of 513 K for four passes and 453 K for four passes, the grain size is further reduced compared to the single-step ECAP process, with average grain size $\sim$0.8 μm. The grain size distribution is also more homogenous, with more than 80% of the grains in the range of 0.5–1.5 μm.

The misorientation data of the ECAP processed ZK60 alloys are shown in Fig. 4. The results show that both alloys after single-step and two-step ECAP process tend to form a grain structure with high grain boundaries. After ECAP eight passes at 513 K, most grain boundaries are high angle boundaries (HABs). The average misorientation is 43.8°. It is interesting to note that misorientation distribution of the single-step ECAP processed alloy exhibits a bi-model type. Two peaks located at around 30° and 90° were observed. This kind of characteristic was also

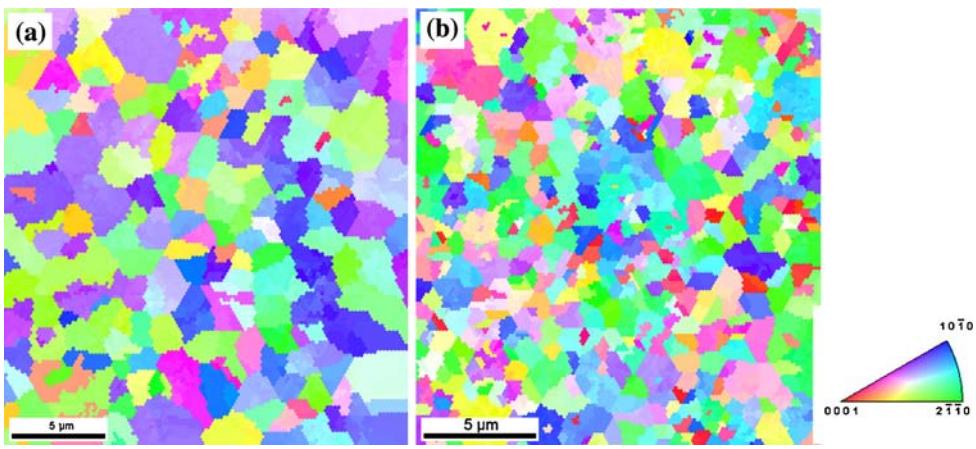

Fig. 2 OIM mapping of the ZK60 alloys processed by single-step ECAP at 513 K for eight passes (**a**) and two-step ECAP at 513 K for four passes and 453 K for four passes (**b**)

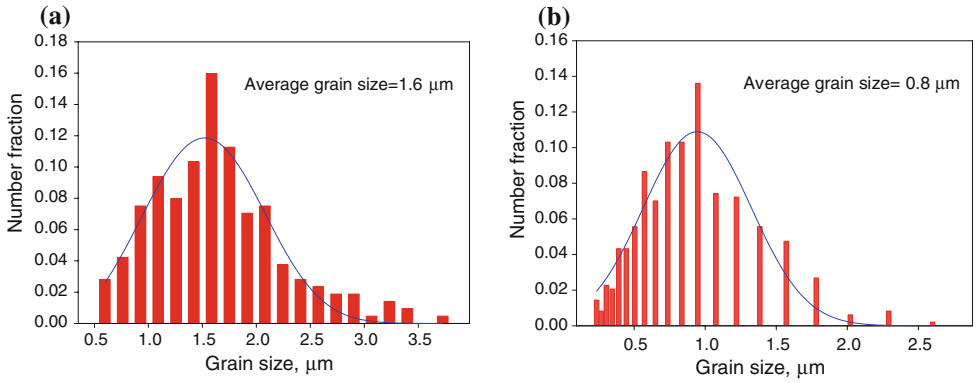

Fig. 3 The grain size distribution of the ZK60 alloy processed by single-step ECAP at 513 K for eight passes (**a**) and two-step ECAP at 513 K for four passes and 453 K for four passes (**b**)

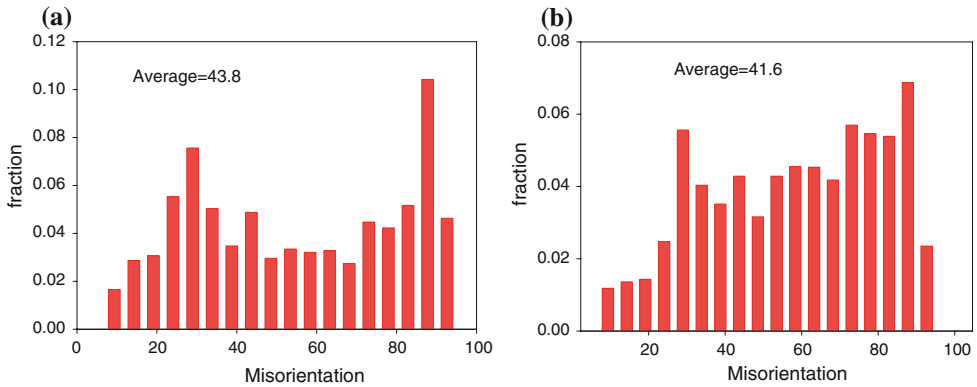

Fig. 4 The misorientation distribution of the ZK60 alloys processed by single-step ECAP at 513 K for eight passes (**a**) and two-step ECAP at 513 K for four passes and 453 K for four passes (**b**)

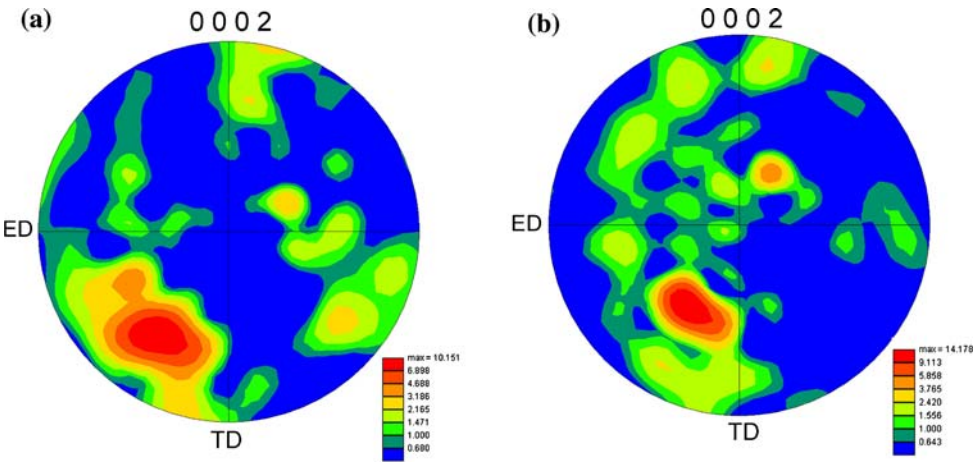

Fig. 5 {0002} pole figures of the ZK60 alloys processed by single-step ECAP at 513 K for eight passes (**a**) and two-step ECAP at 513 K for four passes and 453 K for four passes (**b**)

reported on AZ31 alloy fabricated by ECAP and cyclic extrusion [24, 25]. However, the formation mechanism of this phenomenon is still unclear yet. However, the distribution becomes more homogenous after the two-step ECAP process, though the average misorientation slightly decreases to 41.6°.

Figure 5 shows the {0002} pole figures of the ZK60 alloys after single-step and two-step ECAP process. It can be seen that both alloy shows a similar texture. The maximum pole intensity was located at nearly 45° from extrusion direction (ED) direction toward transversal direction (TD). The texture results are consistent with the geometry of the ECAP die, where the shear direction is 45° with the extrusion direction. After two-step ECAP process, the maximum pole intensity slightly increased compared to single-step ECAP process. The texture also becomes less spread compared to the single-step ECAP process. The texture intensity pole after two-step ECAP process also starts to incline to the TD direction. It is necessary to note that the texture intensity pole in both alloys has a trend to incline toward the pole axis, which resulting into a soft orientation to the extrusion direction.

TEM microstructure

Figure 6 shows the TEM microstructure of the ECAPed ZK60 alloys after single-step ECAP processing. After ECAP at 513 K for four passes, a high density of dislocation was introduced into the material, as shown in Fig. 6a. The microstructure of the alloy consists of equiaxed grains with high dislocation density. However, this kind of high density dislocation is unstable and it can readily transform to subgrain structure with low angle grain boundaries, as shown in Fig. 6b. Figure 6c shows the microstructure after ECAP for eight passes at 513 K. It can be seen that a well-defined grain structure has formed. The grain interior dislocation density was dramatically decreased compared to that of four passes. It is possible that most dislocations formed during ECAP have been absorbed by subgrain boundaries, leading to the decrease of grain interior dislocations and increase of grain boundary misorientation. Some coarse secondary precipitates were observed within grain interior and along the grain boundaries. According to the investigation of Pan and colleagues [26–28], the coarse particles might be $MgZn_2$, which was descended from the solidification process. The fine particle might be MgZn, which precipitate during the ECAP. These precipitates are believed to be effective in impeding grain boundary mobility and thereby restrict the development of grain growth.

Figure 7 shows the TEM micrographs of the microstructure of ZK60 alloy after two-step ECAP process. After low temperature ECAP at the second step, the high density of dislocation was retained within the alloy. The grain boundaries became vague due to the high internal stress introduced by the severe plastic deformation. Compared to the single-step ECAP process, the two-step ECAP process produces a more refined grain structure, with grain size <1 μm. It is necessary to note that some deformation twins were observed after two-step ECAP process, showing that twining also played as an important assistant mechanism during low temperature ECAP.

Mechanical properties

Representative stress–strain curves of ECAP processed ZK60 alloy at room temperature are shown in Fig. 8. The

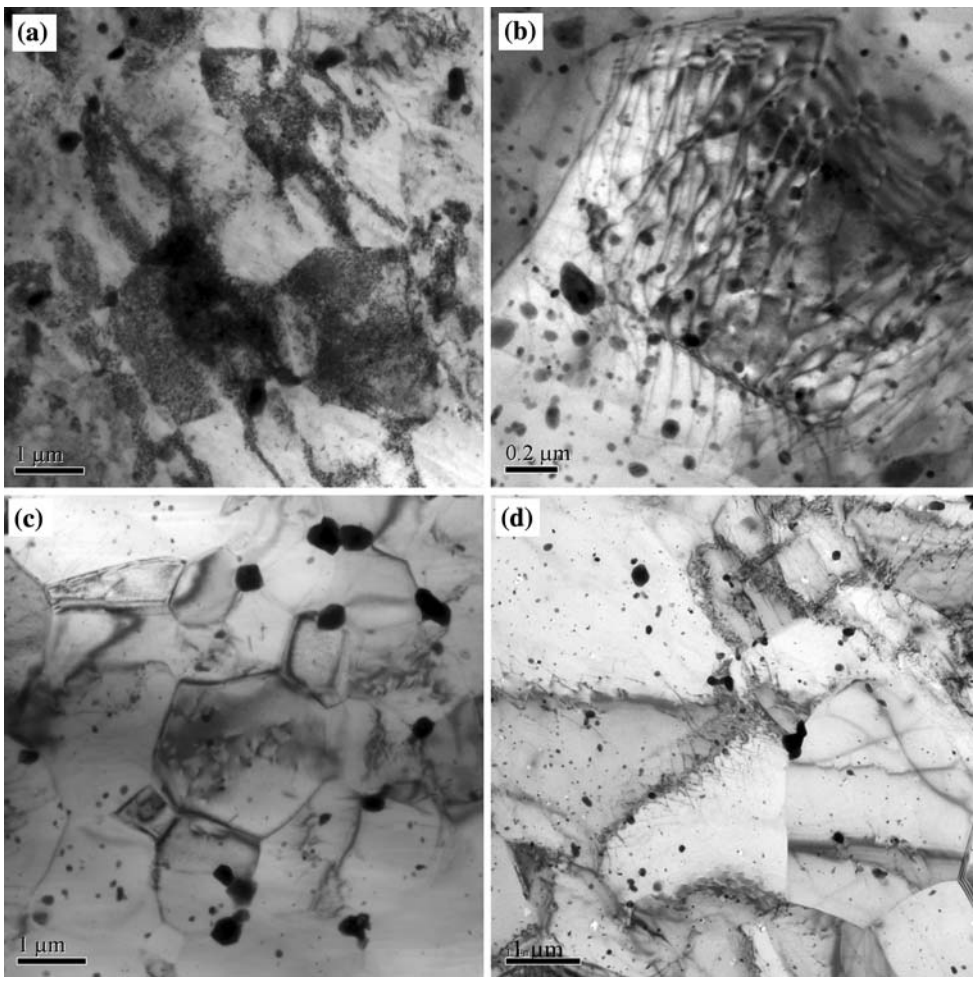

Fig. 6 The grain structure and dislocation configurations of ZK60 alloys after single-step ECAP at 513 K for four passes (**a**), (**b**) and eight passes (**c**), (**d**)

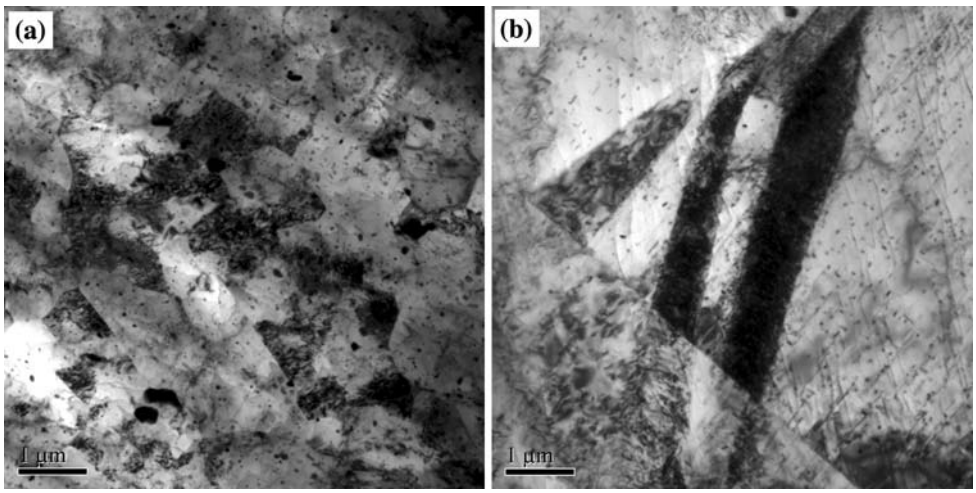

Fig. 7 The grain structure (**a**) and deformation twins (**b**) of ZK60 alloys after two-step ECAP at 513 K for four passes and 453 K for four passes

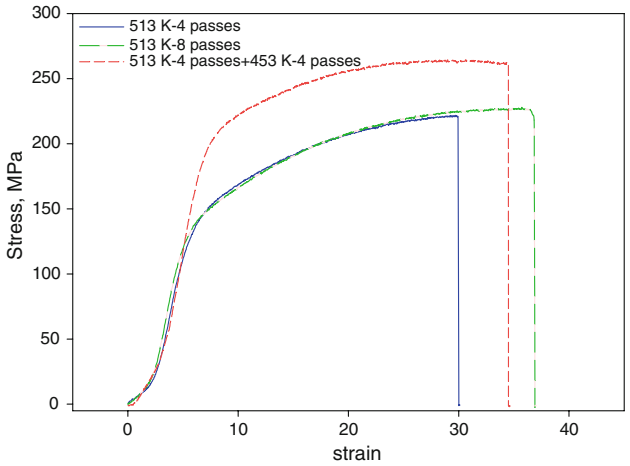

Fig. 8 Room temperature mechanical properties of the ZK60 alloys after ECAP processing

Table 1 Room temperature mechanical properties of the ZK60 alloys after ECAP process

Sample	Ultimate tensile strength (MPa)	Yield strength (MPa)	Elongation to failure (%)
513 K-four passes	221	120	22.2
513 K-eight passes	226	125	28.9
513 K-four passes + 453 K-four passes	266	175	25.9

values of the tensile yield stress, the ultimate tensile stress, and the elongation to failure are summarized in Table 1. For the single-step ECAP alloys, no significant change on strength was observed when the pressing pass increased from 4 to 8. However, the elongation to failure has obviously increased with the increasing pressing pass. It can be seen that the two-step ECAP process can significantly increase both yield strength and ultimate tensile strength compared to the alloy ECAP processed at 513 K. The elongation to failure was also improved compared to the alloy ECAP processed at 513 K for four passes but still lower than that of the alloy processed at 513 K for eight passes.

Discussion

The results obtained in this investigation prove that ECAP produces a substantial grain refinement in the ZK60 alloy. The two-step ECAP process allows the ZK60 alloy be ECAP deformed at low temperature and is more effective in grain refinement than the single-step ECAP process. However, the grain refinement process during the ECAP process is complicated. Though many grain refinement mechanisms have been proposed [29–32], no universal one can be achieved. For magnesium alloys, many researchers attribute the grain refinement to the dynamic recovery and recrystallization, where the new grain size nucleate at the site of the original grain boundaries. However, due to the high temperature of ECAP process for magnesium alloys, the non-basal slip systems are easily activated. Therefore, cross-slip occurs and this generates a complicated dislocation network, as shown in Fig. 6a. In order to reduce energy, this kind of dislocation network can easily rearrange into dislocation interface or low angle grain boundaries, as shown in Fig.6b. According to Baik et al. [33], the average subgrain size d is directly related to the total dislocation density through:

$$d = \frac{K}{\sqrt{\rho_t}},$$

where ρ_t is the total dislocation density, K is a constant which is dependent on the total dislocation density. During the deformation of ECAP, the dislocation density can be

separated into two aspects, i.e., dislocations forming a cell structure and those contained within the cell interiors. Thus, the total dislocation density can be described as:

$$\rho_t = f\rho_w + (1-f)\rho_c,$$

where f denotes the volume fraction of the cell walls, ρ_w and ρ_c are the dislocation density of the cell wall and the cell interior, respectively. According to the previous report [33], with the increasing strain, the fraction of the cell walls f increase. At the initial stage of ECAP, as a result of the activation of multi-slip system at high temperature, a high dislocation density was introduced into the ZK60 alloy. Therefore, a high fraction of ρ_c was obtained, which resulted in a rapid grain refinement during the first four passes. However, this structure with high density of dislocations is metastable, the dislocations can be readily rearranged into cell structure and dislocations walls, as shown in Fig. 6b. With increasing strain, the new generated dislocations and interior dislocations were gradually absorbed into the low grain boundaries, leading to a dramatic decrease of the interior dislocations, as shown in Fig. 6d. This leads to the increase of ρ_w and decrease of ρ_c, and the total dislocation density nearly keep unchanged. Therefore, after eight passes, though well-defined grain boundaries were attained, the grain size was not further reduced. However, the cell interior dislocation density was raised again after two-step ECAP process where additional four passes were carried out at 453 K, as shown in Fig. 7a. The increased dislocation density is mainly related to the low recovery rate at low temperature. Therefore, a further grain refinement was achieved after the two-step ECAP process at low temperature.

The results also show that a significant improvement on room temperature mechanical properties after the two-step ECAP process. The mechanical properties of the ECAP processed alloys are largely determined by grain structure and texture. Kim et al. [34–36] has reported an abnormal decrease of strength with decreasing grain size, which was against Hall–Petch equation. They ascribed this phenomenon to the texture variation during the ECAP process. However, in the present investigation, the texture after single-step and two-step ECAP process is similar. Both alloy shows a strong {0002} texture. It is suggested that the texture difference has minor influence on these two ECAP process alloys. Therefore, the increase on the strength may mainly be ascribed to the significant grain refinement after low temperature deformation in two-step ECAP process. In addition, due to the low recovery rate at low temperature, more dislocations would be retained in the alloy after two-step ECAP process. Severe dislocation entanglements were generated due to the interactions of these dislocations, as shown in Fig. 7a. The entanglements can act as barriers for dislocation movement and may also contribute to the improvement of the mechanical properties.

Summary and conclusion

The grain structure and room temperature mechanical properties of the ZK60 alloy after ECAP processing were investigated. The following conclusions can be drawn.

1. ECAP processing is effective in producing fine-grained ZK60 alloys. For single-step ECAP process, the grain size reduction is limited by increasing the pressing pass from 4 to 8. Compared to single-step ECAP, the two-step ECAP process is more effective in grain refinement due to the lower deformation temperature. A grain size of $\sim$0.8 μm can be achieved after the two-step ECAP processing.
2. For single-step ECAP process, increasing the pressing pass has minor influence on the strength of the ECAP alloy but increase the elongation to failure. Compared to the single-step ECAP process, the tensile strength of the two-step ECAP processed alloy has largely improved.
3. Both alloy after single-step and two-step ECAP process exhibits similar strong {0002} texture. The strength improvement after the two-step ECAP process is mainly ascribed to the grain refinement.

References

1. Hockauf M, Meyer L, Nickel D, Alisch G, Lampke T, Wielage B, Krüger L (2008) J Mater Sci 43(23):7409. doi:10.1007/s10853-008-2724-9
2. Meyer L, Sommer K, Halle T, Hockauf M (2008) J Mater Sci 43(23):7426. doi:10.1007/s10853-008-2725-8
3. Semenova I, Valiev R, Yakushina E, Salimgareeva G, Lowe T (2008) J Mater Sci 43(23):7354. doi:10.1007/s10853-008-2984-4
4. Sivaraman A, Chakkingal U (2008) J Mater Sci 43(23):7432. doi:10.1007/s10853-008-2871-z
5. Swaminathan S, García-Infanta J, McNelley T, Ruano O, Carreño F (2008) J Mater Sci 43(23):7501. doi:10.1007/s10853-008-2625-y
6. Zhilyaev A, Swaminathan S, Gimazov A, McNelley T, Langdon TG (2008) J Mater Sci 43(23):7451. doi:10.1007/s10853-008-2714-y
7. Dinkel M, Pyczak F, May J, Höppel H, Göken M (2008) J Mater Sci 43(23):7481. doi:10.1007/s10853-008-2859-8
8. Lim CY, Jung JH, Man SZ (2004) Mater Sci Forum (449–452):177
9. Ma X, Lapovok R, Gu C, Molotnikov A, Estrin Y, Pereloma EV, Davies CHJ, Hodgson PD (2009) J Mater Sci 44(14):3807. doi:10.1007/s10853-009-3515-7
10. Kumar P, Xu C, Langdon TG (2009) J Mater Sci 44(14):3913. doi:10.1007/s10853-009-3535-3
11. Figueiredo R, Langdon TG (2008) J Mater Sci 43(23):7366. doi:10.1007/s10853-008-2846-0

12. Lapovok R, Estrin Y, Popov M, Rundell S, Williams T (2008) J Mater Sci 43(23):7372. doi:10.1007/s10853-008-2685-z
13. Chuvil'deev VN, Nieh TG, Gryaznov MY, Sysoev AN, Kopylov VI (2004) Scr Mater 50(6):861
14. Xia K, Wang JT, Wu X, Chen G, Gurvan M (2005) Mater Sci Eng A (410–411):324
15. Watanabe H, Mukai T, Ishikawa K, Higashi K (2002) Scr Mater 46(12):851
16. Matsubara K, Miyahara Y, Horita Z, Langdon TG (2003) Acta Mater 51(11):3073
17. Jin L, Lin DL, Mao DL, Zeng XQ, Ding WJ (2005) Mater Lett 59(18):2267
18. Figueiredo RB, Langdon TG (2009) J Mater Sci 44(17):4758. doi:10.1007/s10853-009-3725-z
19. Figueiredo RB, Langdon TG (2009) Mater Sci Eng A 503 (1–2):141
20. Li B, Ma E, Ramesh KT (2008) Metall Mater Trans A 39A(11):2607
21. Lapovok RC, Thomson PF, Estrin Y (2005) J Mater Res 20(6):1375
22. Chuvil'deev V, Nieh TG, Gryaznov MY, Kopylov VI, Sysoev AN (2004) J Alloy Compd 378(1–2):253
23. Figueiredo RB, Langdon TG (2006) Mater Sci Eng A 430 (1–2):151
24. Jin L, Lin DL, Mao DL, Zeng XQ, Ding WJ (2006) J Alloy Compd 426(1–2):148
25. Chen YJ, Wang QD, Roven HJ, Karlsen M, Yu YD, Liu MP, Hjelen J (2008) J Alloy Compd 462(1–2):192
26. Pan FS, Wang WM, Ma YL, Zuo RL, Tang AT, Zhang J (2005) Mater Sci Forum (488–489):181
27. Singh A, Tsai AP (2007) Scr Mater 57(10):941
28. Gao X, Nie JF (2007) Scr Mater 56(8):645
29. Iwahashi Y, Horita Z, Nemoto M, Langdon TG (1998) Acta Mater 46(9):3317
30. Su CW, Lu L, Lai MO (2006) Mater Sci Eng A 434(1–2):227
31. Xu C, Furukawa M, Horita Z, Langdon TG (2005) Mater Sci Eng A 398(1–2):66
32. Zhu YT, Lowe TC (2000) Mater Sci Eng A 291(1–2):46
33. Baik SC, Estrin Y, Kim HS, Hellmig RJ (2003) Mater Sci Eng A 351(1–2):86
34. Kim WJ, An CW, Kim YS, Hong SI (2002) Scr Mater 47(1):39
35. Kim WJ, Hong SI, Kim YS, Min SH, Jeong HT, Lee JD (2003) Acta Mater 51(11):3293
36. Kim WJ, Jeong HT (2005) Mater Trans 46(2):251